Volume 60
Number 33
28 April 2024
Pages 4373–4500

ChemComm

Chemical Communications

rsc.li/chemcomm

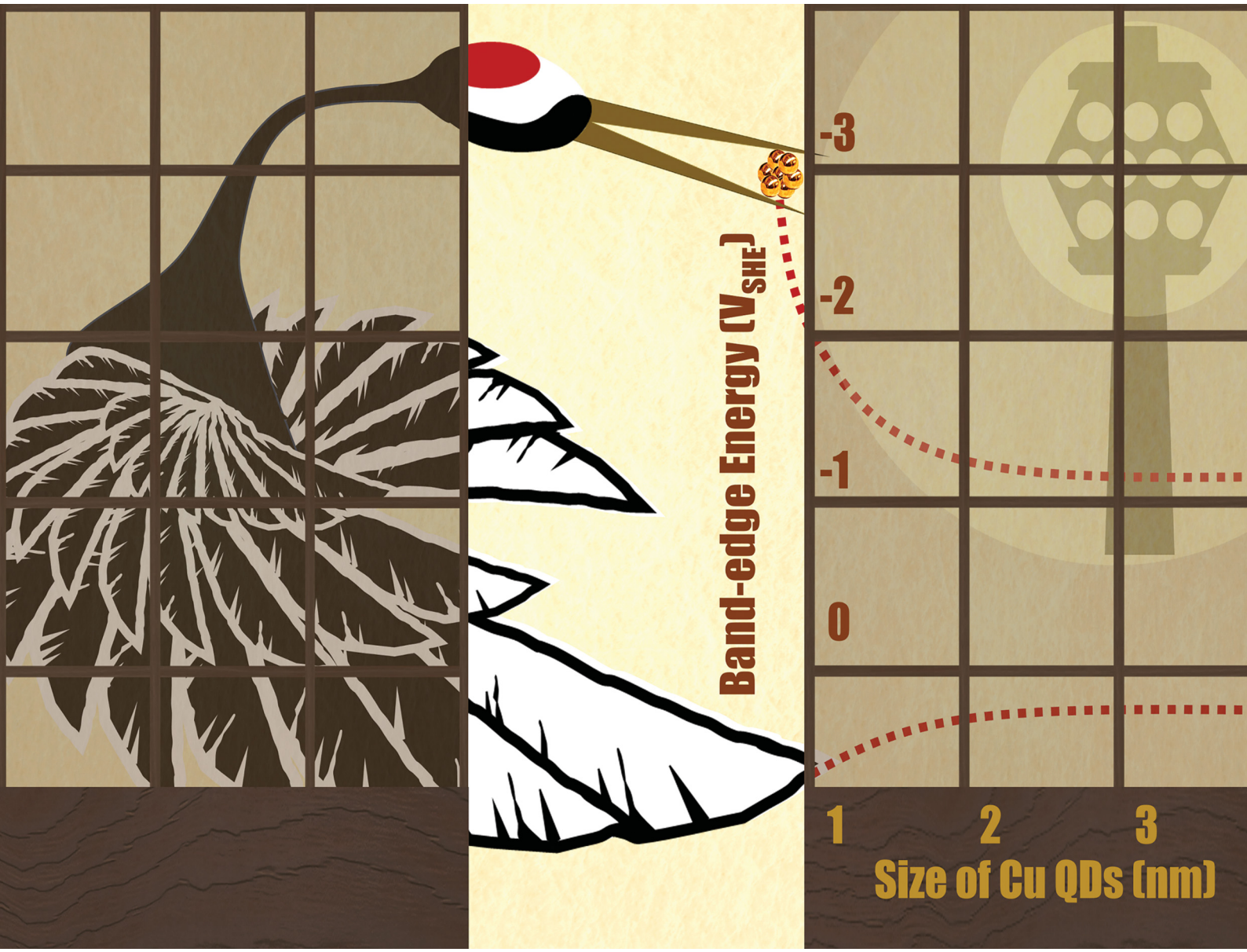

ISSN 1359-7345

ROYAL SOCIETY OF CHEMISTRY

COMMUNICATION

Hiroto Watanabe, Hiroaki Imai *et al.*

The size-dependent valence and conduction band-edge energies of Cu quantum dots

60 YEARS ANNIVERSARY

ChemComm

COMMUNICATION

View Article Online
View Journal | View Issue

Check for updates

Cite this: *Chem. Commun.*, 2024, **60**, 4419

Received 18th January 2024,
Accepted 12th March 2024

DOI: 10.1039/d4cc00260a

rsc.li/chemcomm

The size-dependent valence and conduction band-edge energies of Cu quantum dots†

Takahiro Matsui,[a] Hiroto Watanabe, *[a] Shoichi Somekawa,[b] Sayaka Yanagida,[b] Yuya Oaki [a] and Hiroaki Imai *[a]

Ultra-small metal particles having band gaps are regarded as a new class of functional materials. We investigated the size dependencies of the band-edge energies on Cu quantum-dots in the size range of 0.7–2.1 nm. The extremely high conduction band-edge energies owing to the strong quantum-size effects were observed for sizes below 1 nm.

A shiny luster, which originates from the light reflection by their free electrons, is one of the most common characteristics of metals.[1] The continuous energy band of metals around their Fermi level allows the presence of free electrons. When the particle sizes are reduced to a few tens of nanometers, the collective oscillation of the free electrons resonates with visible light and displays brilliant colors, which is called localized surface plasmon resonance (LSPR) (Fig. 1a).[2] Upon further reduction of the particle size to near their Fermi wavelength (~0.5 nm for Au), their optical and electronic properties change dramatically.[3] In this size region, the electronic structure changes from a metallic to a molecule-like state (Fig. 1c). LSPR absorption is no longer observable due to the absence of free electrons and new absorption edges that originate from the electronic transition across the energy-gap.[4] In the earlier studies, these tiny particles, mostly called "metal clusters," were only formed as a cluster ion beam in a vacuum chamber.[4b] Since these metal clusters are formed and exist only for a short time in the chamber, their research has been limited to the field of fundamental physical chemistry.[4b,5] Recently, metal clusters were regarded as practical materials owing to the development of large-scale synthetic routes *via* solution processes.[6] Thus, these tiny metal clusters are now gathering interest in the field of materials chemistry as a new class of fluorophores and photocatalysts. For example, thiol-protected Au clusters are one of the most studied species.[6a,b] They show size-dependent photoluminescence in the UV and near-infrared regions. For Au, the transition from the metallic to the molecule-like state occurs at a size of ~1.6–1.8 nm (Au_{144}–Au_{187}).[7] Thus, the appearance of energy-gap states is not only the case for 2-dimensional clusters having a few-atoms, but also occurs for much larger 3-dimensional particles having a few tens to a few hundreds of atoms. These particles were recognized as metal quantum-dots (QDs) (Fig. 1b).[3a]

From the viewpoint of solid-state physics, the formation of electronic gap states with the size reduction of the metal particles is ascribed to quantum size effects, which have been well studied in the field of semiconductors.[8] When the sizes of

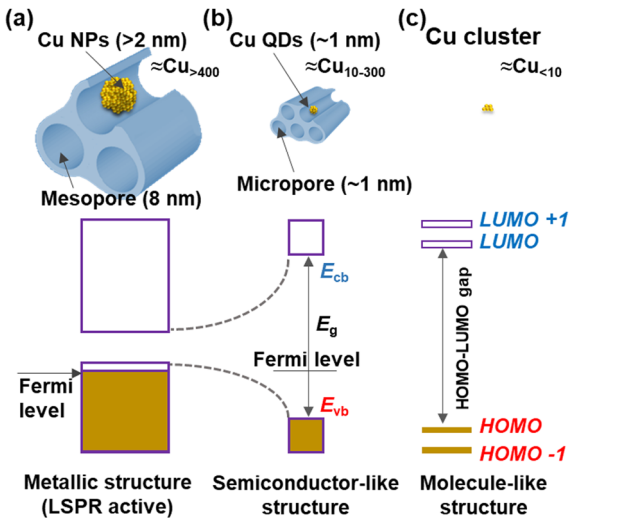

Fig. 1 Schematic illustration of Cu nanoparticles (Cu NPs), Cu quantum dots (Cu QDs) and Cu clusters.

[a] *Department of Applied Chemistry, Faculty of Science and Technology, Keio University, 3-14-1 Hiyoshi, Kohoku-ku, Yokohama 223-8522, Japan. E-mail: hiroaki@applc.keio.ac.jp*

[b] *Tokyo Metropolitan Industrial Technology Research Institute, 2-4-10 Aomi. Koto-ku, Tokyo 135-0064, Japan*

† Electronic supplementary information (ESI) available: (1) Materials. (2) Preparation and characterization of porous silicas. (3) Preparation and characterization of the CuO QDs and Cu QDs. (4) Particle size analysis of the CuO QDs and Cu QDs. (5) Determination of the valence states of the CuO QDs and Cu QDs by X-ray absorption near-edge structure measurements. (6) Determination of the band structures of the CuO QDs and Cu QDs. (7) Curve fitting with effective mass approximation (EMA) for the CuO QDs and Cu QDs. See DOI: https://doi.org/10.1039/d4cc00260a

Open Access Article. Published on 13 March 2024. Downloaded on 1/14/2026 8:37:21 PM. This article is licensed under a Creative Commons Attribution-NonCommercial 3.0 Unported Licence.

Open Access Article. Published on 13 March 2024. Downloaded on 1/14/2026 8:37:21 PM.
This article is licensed under a Creative Commons Attribution-NonCommercial 3.0 Unported Licence.

the semiconductor particles are similar to their exciton Bohr radius, their band gap energies (E_gs) increase with the size reduction. Therefore, the E_g of QDs is controlled by changing their particle sizes. Semiconductor QDs show size-dependent functionalities, such as color-tunable bright luminescence.[9–12]

In the field of photocatalysis, valence and conduction band-edge energies (E_{vb} and E_{cb}) are important because the photocatalytic activity strongly depends on the alignment of their energies and the redox potential of the target reactions.[8b,13] Therefore, the photocatalytic reactivities are controllable by changing the sizes of the QDs. For example, the E_{vb} and E_{cb} of WO_3 QDs were optimized by controlling their sizes below 1 nm to improve the photocatalytic hydroxylation of benzene.[14] The size dependency of E_{vb} and E_{cb} owing to the quantum size effect is theoretically calculated using an effective mass approximation (EMA) method and shows good agreement with experimental values.[15]

The aim of the present study is to determine the size dependency of the E_{vb} and E_{cb} of Cu QDs by using spectroscopic approaches. Different from Au and Pt, Cu has a relatively high Fermi level in its bulk state.[16] Thus, Cu QDs smaller than 1 nm are excellent candidates for photocatalysts having a high E_{cb} level. Although the size dependency of the E_{vb} and E_{cb} of Cu QDs has been theoretically investigated,[17] experimental work was lacking because of the difficulty of the size-selective synthesis. Previously, our research group found a large expansion of E_g for CuO QDs with sizes below 1 nm, which were synthesized by using pores of porous silicas (PSs) as templates.[18] In the present study, we synthesized Cu QDs through the reduction of CuO QDs and then unveiled the size dependency of the E_{vb}, and E_{cb} of the Cu QDs (Fig. 1). In particular, for the 1 nm Cu QDs, an extremely high E_{cb} was observed, which corresponded to the high photocatalytic reduction ability of the Cu QDs expected from the theoretical study.[19] Furthermore, we found that the band expansion of the metal QDs was explainable *via* the EMA method by taking into account the physical quantities obtained from a recent spectroscopic study of Cu.[20]

Here, four kinds of PSs with different pore sizes were used as templates for the production of CuO QDs (see Section S2 in the ESI† for the synthesis and analyses of the PSs).[21] CuO QDs were prepared in the PSs using a simple impregnation method (see Section S3 in the ESI† for the experimental details). As shown in the typical transmission electron microscopy (TEM) images (Fig. 2a, and Fig. S3 in the ESI†), fine particles were prepared in the pores of PSs, and the particle size was well controlled in a range from 0.6 to 2.1 nm. The presence of CuO was confirmed by observing a lattice fringe image and a fast Fourier transform (FFT) pattern corresponding to the (111) plane of monoclinic CuO (inset in Fig. 2a-i). From UV-visible (UV-vis) absorption spectra, we observed a broad absorption of Cu^{2+} *d–d* transition around 800 nm and size-dependent absorption edges around 300 to 500 nm for CuO QDs (see Fig. 2c, Fig. S8 and S9 in the ESI†). As described in our previous study,[18] the band gap energy of the CuO QDs increased remarkably owing to the strong quantum size effect expressed below 2 nm. The detailed band structure analyses of the CuO QDs are described in Section 6 in the ESI.†

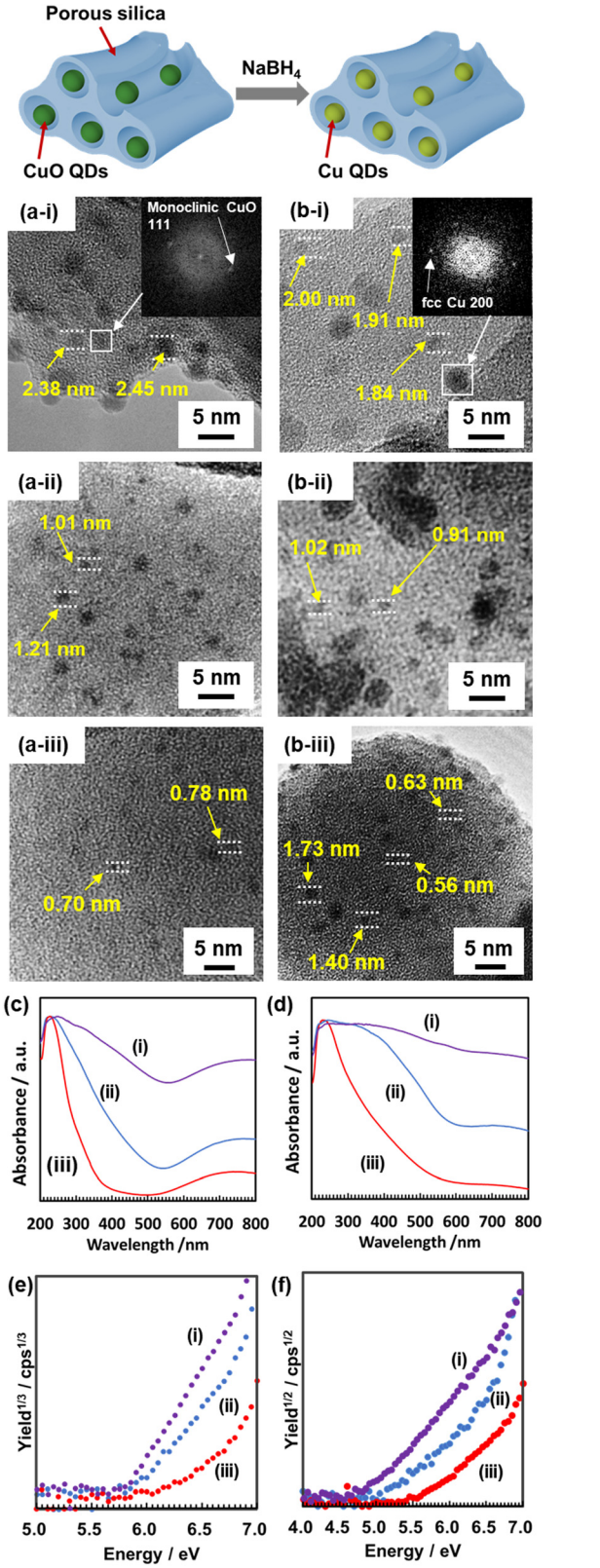

Fig. 2 Typical TEM images (a) and (b), UV-vis spectra (c) and (d), and PYSA (e) and (f) of CuO QDs, (a), (c) and (e) and Cu QDs (b), (d) and (f) prepared (i) in C18PS with 5 M solution, (ii) in C18PS with 0.2 M solution, and (iii) in C6PS with 0.05 M solution.

This journal is © The Royal Society of Chemistry 2024

Open Access Article. Published on 13 March 2024. Downloaded on 1/14/2026 8:37:21 PM.
This article is licensed under a Creative Commons Attribution-NonCommercial 3.0 Unported Licence.

For the Cu QD preparation, a reductant solution of $NaBH_4$ was injected into the pores of PSs containing CuO QDs. Fig. 2b and Fig. S4 in the ESI† show typical TEM images of Cu QDs. In particular, for Cu QDs, the aggregation and growth of the particles occurred during the high magnitude TEM observations (Fig. S5 in the ESI†). We analyzed the particle size distribution profiles by deconvoluting the primal and large particles formed by electron beam exposure to determine the average size and dispersity of the primal particles from TEM images. The primal particle size of the Cu QDs was well controlled in the range from 0.7 to 2.1 nm. As shown in the inset of Fig. 2b-i, we observed a lattice fringe image and an FFT pattern corresponding to the (200) planes of fcc Cu for the sample after the reduction. This clearly indicates the successful formation of Cu QDs. The presence of Cu QDs was also confirmed by the X-ray absorption near-edge structure (XANES) spectra of the samples before and after the reduction (Fig. S7 in the ESI†). The present Cu QDs show no fluorescence due to the absence of surface passivation agents.

The UV-vis spectra indicate that the absorption energy shifts due to the quantum size effect (Fig. 2d and Fig. S10a in the ESI†). After the reduction, the absorption of the Cu^{2+} *d–d* transition disappeared, and the absorption edges shifted to a lower-energy side. These changes in the UV-vis spectra also indicate the reduction of CuO QDs to Cu QDs. The size dependency of the band gap energies of the Cu QDs was calculated using Tauc plots[22] (Fig. S10b in the ESI†) as shown in Fig. 3a. The dotted curve in Fig. 3a represents the theoretical fitting of the present experimental data using an EMA method (see Section S7 in the ESI† for detailed analyses using the EMA method). Adopting a value of $\mu = 1.15\ m_0$ as a reduced mass of Cu, the present experimental data were well fitted using the EMA method. For the 2.1 nm Cu particles, the absorption peak assigned to the LSPR was observed at 580 nm (Fig. S11 in the ESI†).[23] Based on this result, the transition from the metallic state (= LSPR active) to the semiconductor-like state occurs at around 2 nm. This threshold diameter is slightly larger than that of the thiolate-protected Au QDs (1.6–1.8 nm).[7]

For the band-structure analysis of the Cu QDs, their E_{vb} was measured using photoemission yield spectroscopy in air (PYSA) (Fig. 2f and Fig. S13 in the ESI†) (Fig. 2e and Fig. S12 in the ESI† show the PYSA spectra for CuO QDs).[24] PYSA is a powerful tool for investigating the E_{vb} for semiconductors and the Fermi level for metals. The PYSA stimulation with very weak UV light (10–100 nW, 4.0–7.0 eV) under ambient conditions is a suitable method to determine the E_{vb} of QDs, which is sensitive to the measurement conditions.[24b] By combining the E_g obtained from UV-vis spectra and the E_{vb} obtained from PYSA, the size dependency of the E_{vb} and E_{cb} of Cu QDs was obtained and is summarized in Fig. 3b (see Section S6 in the ESI† for detailed analyses). Both the E_{vb} and E_{cb} show dramatic shifts below 1 nm. The energy shift of the E_{cb} is larger than that of the E_{vb}. This is in contrast to the case of CuO QDs (Fig. S14 in the ESI†). The present experimental values were fitted *via* EMA separately for the E_{vb} and E_{cb}. Since the electronic configuration of a Cu atom is described as $1s^2\ 2s^2\ 2p^6\ 3s^2\ 3p^6\ 3d^{10}\ 4s^1\ 4p^0$, the

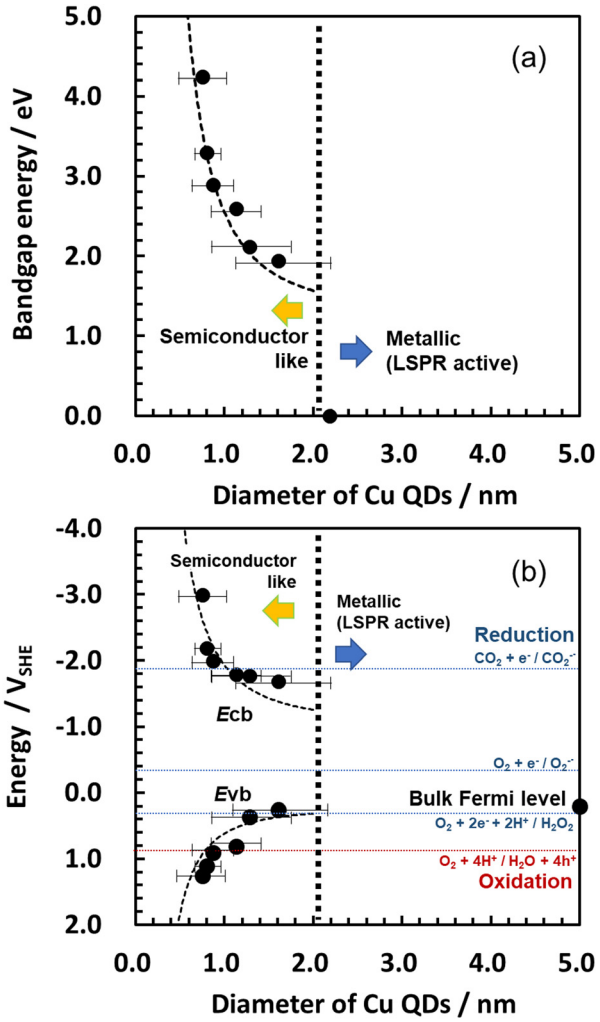

Fig. 3 Size dependency of (a) E_g, (b) E_{vb}, and E_{cb} for Cu QDs. The dotted curves represent calculation data using an EMA method. Several redox potentials of photocatalytic reactions are represented with horizontal lines. The error bars represent the FWHM of the particle size distribution profiles shown in Fig. S4 (ESI†).

partially filled 4s orbitals mainly contribute to the occupied energy state around the Fermi level.[17b] When the quantum size effect became significant, this orbital shifts to the lower-energy side and forms a valence band. On the other hand, unoccupied energy states, which are mainly formed by 4p orbitals, exist above the Fermi level. Recently, Sonoda found that the lowest unoccupied bulk electronic state of Cu lies 1.24 eV above the Fermi level (structure D in the article) by using angle-resolved two-photon photoemission spectroscopy.[20] This energy state shifts to the higher-energy side and constructs the conduction-band edge owing to the quantum size effect. The effective mass of the electron in this state was estimated to be 1.67 m_0. Therefore, we used the following physical quantities for the EMA fitting: $E_{cb(bulk)} = -1.03\ V_{SHE}$, $E_{vb(bulk)} = +0.21\ V_{SHE}$, $m_e = 1.67\ m_0$, $\mu = 1.15\ m_0$, and $m_h = 3.69\ m_0$ (see Section S7 in the ESI† for details of the EMA method). Using these values, the present experimental data were well fitted with EMA (Fig. 3b). Therefore, similar to the semiconductor QDs, the formation of

Open Access Article. Published on 13 March 2024. Downloaded on 1/14/2026 8:37:21 PM.
This article is licensed under a Creative Commons Attribution-NonCommercial 3.0 Unported Licence.

the band gap states and their expansion due to the size reduction of metal QDs are explainable with a theory based on the quantum size effects of nanoparticles. The present results show a similar tendency with previous studies.[4b,19b]

Here, the E_{cb} for 1 nm QDs exceeds −2.0 V_{SHE} and shifts to −3.0 V_{SHE} for 0.7 nm Cu QDs. These E_{cb} values are higher than those of the single-electron reduction potential of O_2 (−0.35 V_{SHE})[25] and CO_2 (−1.90 V_{SHE}).[26] Thus, as described in the previous molecular orbital calculations, Cu QDs are efficient photocatalysts, especially for the reduction reaction. Cysteine-capped Cu_{10} was reported to have high photocatalytic activity for the degradation of an organic dye.[19b] This is probably due to the high E_{cb}, which produces highly active superoxide radicals. The Cu_{10} also has high stability against aerobic oxidation owing to its low HOMO level expected in the previous study.[19b] In the present study, we experimentally observed the low E_{vb} levels (+ 1.26 V_{SHE}), which were located below the reduction potential of molecular oxygen for 0.7 nm Cu QDs.[25] Taking the relationship between the E_{vb} and the particle sizes into account, oxidative stability is expected for Cu QDs smaller than 2 nm. However, the E_{vb} levels of the Cu QDs were only slightly lower than the oxidation potential of water.[25] Thus, relatively low efficiency is expected for the photocatalytic water oxidation. The construction of a Z-scheme heterojunction[27] with oxide semiconductors is required for the best photocatalytic performance of the Cu QDs.

In summary, we produced Cu QDs of various sizes, ranging from 0.7 to 2.1 nm, by reducing CuO QDs synthesized in the pores of PSs. The size dependency of their E_{vb} and E_{cb} was investigated experimentally using UV-vis and PYSA techniques. We observed a significant shift in the E_{vb} and E_{cb}, which was due to strong quantum size effects when the particle sizes were below 1 nm. Since the E_{cb} for 0.7 nm Cu QDs exceeds the single-electron reduction potentials of O_2 and CO_2, Cu QDs would be potential candidates for efficient photocatalysts for the reduction reactions.

We thank Dr Y. Nakajima (RIKEN KEIKI Co., Ltd.) for helpful discussions and kind assistance with the PYSA experiments. We thank Dr T. Kaya (Keio University) for the TEM experiments. This work was partially supported by JSPS KAKENHI grant number JP21H01627.

Conflicts of interest

There are no conflicts to declare.

Notes and references

1 M. A. White, *Physical Properties of Materials*, CRC Press, Boca Raton, 2018, pp. 47.
2 K. M. Mayer and J. H. Hafner, *Chem. Rev.*, 2011, **111**, 3828.
3 (*a*) J. Zheng, P. R. Nicovich and R. M. Dickson, *Annu. Rev. Phys. Chem.*, 2007, **58**, 409; (*b*) Y. Lu and W. Chen, *Chem. Soc. Rev.*, 2012, **41**, 3594.
4 (*a*) W. A. de Heer, *Rev. Mod. Phys.*, 1993, **65**, 611; (*b*) K. J. Taylor, C. L. Pettiette-Hall, O. Cheshnovsky and R. E. Smalley, *J. Chem. Phys.*, 1992, **96**, 3319.
5 (*a*) A. Sebetci and Z. B. Güvenç, *Surf. Sci.*, 2003, **525**, 66; (*b*) M. A. Tafoughalt and M. Samah, *Comput. Theor. Chem.*, 2014, **1033**, 23; (*c*) T. Tsuneda, *J. Comput. Chem.*, 2019, **40**, 206.
6 (*a*) J. Zheng, C. Zhang and R. M. Dickson, *Phys. Chem. Lett.*, 2004, **93**, 077402-1; (*b*) K. G. Stamplecoskie and P. V. Kamat, *J. Am. Chem. Soc.*, 2014, **136**, 11093; (*c*) I. Chakraborty, R. G. Bhuin, S. Bhat and T. Pradeep, *Nanoscale*, 2014, **6**, 8561; C. Vázquez-Vázquez, M. Bañobre-López, A. Mitra, M. A. López-Quintela and J. Rivas, *Langmuir*, 2009, **25**, 8208; (*d*) T. Imaoka and K. Yamamoto, *Bull. Chem. Soc. Jpn.*, 2019, **92**, 941.
7 Y. Negishi, T. Nakazaki, S. Malola, S. Takano, Y. Niihori, W. Kurashige, S. Yamazoe, T. Tsukuda and H. Hakkinen, *J. Am. Chem. Soc.*, 2015, **137**, 1206.
8 (*a*) F. P. García de Arquer, D. V. Talapin, V. I. Klimov, Y. Arakawa, M. Bayer and E. H. Sargent, *Science*, 2021, **373**, eaaz8541; (*b*) D. Kandi, S. Martha and K. M. Parida, *Int. J. Hydrogen Energy*, 2017, **42**, 9467.
9 M. L. Landry, T. E. Morrell, T. K. Karagounis, C. H. Hsia and C. Y. Wang, *J. Chem. Educ.*, 2014, **91**, 274.
10 M. Shen, W. Jia, Y. You, F. Li, S. Tian, J. Li, Y. Jin and D. Han, *Nanoscale Res. Lett.*, 2013, **8**, 253.
11 H. R. You, J. Y. Park, D. H. Lee, Y. Kim and J. Choi, *Appl. Sci.*, 2020, **10**, 975.
12 T. Nakotte, H. Luo and J. Pietryga, *Nanomaterials*, 2020, **10**, 172.
13 (*a*) T. Inoue, A. Fujishima, S. Konishi and K. Honda, *Nature*, 1979, **277**, 637; (*b*) T. Suzuki, H. Watanabe, Y. Oaki and H. Imai, *Chem. Commun.*, 2016, **52**, 6185.
14 A. Ohno, H. Watanabe, T. Matsui, S. Somekawa, M. Tomisaki, Y. Einaga, Y. Oaki and H. Imai, *Catal. Sci. Technol.*, 2021, **11**, 6537.
15 (*a*) L. Brus, *J. Phys. Chem.*, 1986, **90**, 2555; (*b*) F. Rodríguez-Mas, J. C. Ferrer, J. L. Alonso, D. Valiente and S. Fernández de Ávila, *Crystals*, 2020, **10**, 226.
16 T. Tani, *J. Soc. Photogr. Imaging Jpn.*, 2015, **78**, 16.
17 (*a*) M. Kabir, A. Mookerjee and A. K. Bhattacharya, *Eur. Phys. J. D*, 2004, **31**, 477; (*b*) C. G. Li, Z. G. Shen, Y. F. Hu, Y. N. Tang, W. G. Chen and B. Z. Ren, *Sci. Rep.*, 2017, **7**, 1345; (*c*) U. J. Rangel-Peña, R. L. Camacho-Mendoza, S. González-Montiel, L. Feria and J. Cruz-Borbolla, *Clust. Sci.*, 2021, **32**, 1155.
18 H. Tamaki, H. Watanabe, S. Kamiyama, Y. Oaki and H. Imai, *Angew. Chem., Int. Ed.*, 2014, **53**, 10706.
19 (*a*) S. Huseyinova, J. Blanco, F. G. Requejo, J. M. Ramallo-López, M. C. Blanco, D. Buceta and M. A. López-Quintela, *J. Phys. Chem. C*, 2016, **120**, 15902; (*b*) S. Huseyinova, J. M. B. Trillo, J. M. Ramallo-López, F. G. Requejo, D. Buceta and M. A. López-Quintela, *Phys. Chem. Chem. Phys.*, 2023, **25**, 6025.
20 Y. Sonoda, *Phys. Rev. B: Condens. Matter Mater. Phys.*, 2011, **83**, 245410.
21 H. Watanabe, K. Fujikata, Y. Oaki and H. Imai, *Microporous Mesoporous Mater.*, 2015, **214**, 41.
22 J. Tauc, *Mater. Res. Bull.*, 1970, **5**, 721.
23 P. Liu, H. Wang, X. Li, M. Rui and H. Zeng, *RSC Adv.*, 2015, **5**, 79738.
24 (*a*) D. Yamashita, Y. Nakajima, A. Ishizaki and M. Uda, *J. Surf. Anal.*, 2008, **14**, 433; (*b*) J. Jasieniak, M. Califano and S. E. Watkins, *ACS Nano*, 2011, **5**, 5888; (*c*) E. O. Kane, *Phys. Rev.*, 1962, **127**, 131.
25 W. H. Koppenol, D. M. Stanbury and P. L. Bounds, *Free Radical Biol. Med.*, 2010, **49**, 317.
26 S. Lu, F. Lou and Z. Yu, *Catalysts*, 2022, **12**, 228.
27 B.-J. Ng, L. K. Putri, X. Y. Kong, Y. W. The, P. Pasbakhsh and S.-P. Chai, *Adv. Sci.*, 2020, **7**, 1903171.

 This journal is © The Royal Society of Chemistry 2024